Agricultural and Forest Meteorology 250–251 (2018) 171–180

Contents lists available at ScienceDirect

Agricultural and Forest Meteorology

journal homepage: www.elsevier.com/locate/agrformet

Water availability controls *Pinus pinaster* xylem growth and density: A multi-proxy approach along its environmental range

Alberto Arzac[a], Vicente Rozas[b], Philippe Rozenberg[c], José M. Olano[b,*]

[a] Institute of Ecology and Geography, Siberian Federal University, 79 Svobodny pr., 660041, Krasnoyarsk, Russia
[b] Área de Botánica, Departamento de Ciencias Agroforestales, EU de Ingenierías Agrarias, iuFOR-Universidad de Valladolid, Campus Duques de Soria, 42004, Soria, Spain
[c] French National Institute for Agricultural Research, UR0588 Unité d'Amélioration Génétique et Physiologie Forestières, Orléans, France

ARTICLE INFO

Keywords:
Cambial activity
Intra-annual density fluctuations (IADF)
Mediterranean climate
Secondary growth
Standardized Precipitation Evapotranspiration Index (SPEI)
Xylem density

ABSTRACT

Deciphering climatic factors limiting cambial activity is critical to forecast the potential of trees to respond to ongoing climatic change. We explored multiple xylem traits, including tree-ring width, inter-annual micro-density variation and intra-annual density fluctuations (IADF), to unveil the climatic factors constraining cambial activity of a Mediterranean conifer (*Pinus pinaster*) along a continental-aridity gradient. Secondary growth responded mainly to water availability, explaining as much as 64.7% of earlywood growth variance for earlywood growth. The continuous and non-overlapping timing of the climatic signals of earlywood and latewood growth reflected a continuous water limitation of secondary growth along the growing season. Drought also had an extraordinary impact on minimum (D_{min}) and maximum (D_{max}) density, with maximal explained variances reaching 47.4% and 39.1%, respectively. D_{min} was negatively associated to water availability during the initiation of earlywood formation, whereas D_{max} responded positively to water availability during two distinct periods: previous winter and the initiation of latewood formation. IADFs in the latewood were quite common along the gradient, occurred in 21–51% of the rings, and responded to episodes of high rainfall and elevated temperature at different phases of latewood formation. Xylem traits identity outperformed site as a driver of climatic signal, revealing the potential of a multi-proxy approach to unveil multiple facets of the xylogenetic cycle. Cambial plasticity, i.e. the ability to adjust the xylogenesis rate and to arrest and resume cambial activity to exploit favorable climatic windows, was critical for *Pinus pinaster* to thrive within wide climatic envelopes. Nevertheless, the pervasive effect of water availability on all analyzed traits indicates that forthcoming reduced precipitation and increased evapotranspiration, as predicted by climate change models, will negatively impact *P. pinaster* secondary growth along its whole environmental range.

1. Introduction

Trees have a pivotal position in CO_2 dynamics, contributing with the largest fraction of photosynthesis in terrestrial ecosystems (Lal, 2008). Moreover, a significant fraction of the fixed carbon is converted into durable compounds and stored as xylem cell walls that act as a carbon reservoir. Higher temperatures and shifts in precipitation patterns associated to climate change will impact photosynthetic and respiratory rates (Frank et al., 2015, affecting carbon gain capacity, but also tree secondary growth (Granda et al., 2013), thus potentially modifying carbon storage patterns. These phenomena may disrupt the role of trees as CO_2 sinks (Frank et al., 2015), compromising this critical ecosystem service.

Understanding how climate constrains xylogenesis is critical to forecast whether trees will be able to provide carbon storage services under future climatic scenarios (IPCC, 2014). Deciphering factors limiting cambial activity along climatic gradients captures the adjustments of species to thrive in a wide range of environmental conditions, predicting its potential adaptive capacity to ongoing climatic change. Ideally, this information could be achieved by monitoring cambial activity of the species along environmental gradients (Camarero et al., 2010; Pérez-de-Lis et al., 2016b; Rossi et al., 2006). Nevertheless, long-term studies of xylem phenology are usually lacking (Antonucci et al., 2017). Information on cambial activity, however, can be mostly inferred by analysing the permanent imprint of cambial activity on xylem structure (Rossi et al., 2006; Fonti et al., 2010).

Abbreviations: D_{max}, maximum ring density; D_{min}, minimum ring density; EW, earlywood width; IADF, intra-annual density fluctuations; LW, latewood width; LW_{adj}, adjusted latewood index; PCA, Principal Component Analysis; RDA, Redundancy Analysis; RW, tree-ring width; SPEI, Standardized Precipitation Evapotranspiration Index

* Corresponding author.
E-mail address: jmolano@agro.uva.es (J.M. Olano).

https://doi.org/10.1016/j.agrformet.2017.12.257
Received 23 May 2017; Received in revised form 3 December 2017; Accepted 19 December 2017
Available online 28 December 2017
0168-1923/

Ring-width series are routinely used to analyze the effects of climate on cambial activity, including their spatio-temporal dimensions (Fonti et al., 2010). Xylem structure stores additional information to tree-ring width (Speer, 2012). Therefore, multi-proxy approaches, including several xylem traits, may improve our insight on the factors controlling cambial activity (Cleaveland, 1986; Olano et al., 2012; Vaganov et al., 2009). Wood density integrates xylem anatomical traits related to mechanical strength, water transport and carbon storage capacities (Chave et al., 2009), with changes in density mirroring climate variability (Camarero et al., 2014; Rosner et al., 2014). Abrupt intra-annual changes in wood density, namely intra-annual density fluctuations (IADF) – also termed as false rings, double rings or multiple rings (Rigling et al., 2001) – echo sharp changes in weather at an intra-annual level (Fritts, 1976; Schweingruber, 1988). IADFs reveal short-term variation in the pace of xylem formation (De Micco et al., 2007), thus providing information on environmental cues on the cambial activity at intra-annual scale (Olano et al., 2015; Zalloni et al., 2016).

In this work, we explored the climatic factors constraining *Pinus pinaster* Ait. cambial activity along a 300 km latitudinal climatic (precipitation and temperature) gradient comprising a significant portion of this species environmental range. *P. pinaster* is a species of interest, since it inhabits a wide diversity of climatic and environmental conditions, from nearly frost-free areas under Atlantic climates with high water availability to Mediterranean continental climates with strong summer drought and long frost periods.

We analyzed the effect of climatic factors through multiple anatomical proxies of cambial activity. We included tree-ring width at annual (ring) and intra-annual (earlywood and latewood) time scales. We also evaluated the climatic control of wood density, including not only the commonly studied maximum wood density (Vaganov et al., 2011), but also minimum density that may have a strong climatic signal of spring conditions in drought-constrained environments (Camarero et al., 2014; Cleaveland, 1986). Finally, we evaluated the occurrence of different types of IADFs (Rozas et al., 2011; Zalloni et al., 2016), reflecting the potential of *P. pinaster* to adjust its cambial activity to changing climatic conditions at both inter- and intra-annual levels.

We hypothesized that water availability would be the major climatic factor constraining *P. pinaster* cambial activity along the climatic gradient with the effect of water limitation permeating all analyzed tree rings traits (Olano et al., 2014). A plastic response of cambial activity would allow encompass to the range of climatic conditions along the gradient by adjusting its timing to benefit from favorable periods. Finally, we explored the potential of microdensitometric time series as climatic proxies in Atlantic and Mediterranean environments.

2. Materials and methods

2.1. Study area and study species

We sampled four *Pinus pinaster* forest sites along a 300 km North-South gradient of increasing elevation, continentality and summer drought stress in Northern Spain, ranging from oceanic climate conditions at the Spanish Cantabrian Coast to continental climate at the Central Iberian Range (Fig. 1). First site was located at 33 m asl in the Cantabrian Coast (S1, Azkorri, Bizkaia, 43°22'40"N, 3° 0'42"W), with a mean annual temperature of 14.4 °C and a total annual precipitation of 1183 mm, on parent rock of Cretaceous flysch. Second site was located at 750 m asl in the Alto Ebro (S2, Oña, Burgos; 42°45'39"N, 3°25'58"W), with a mean annual temperature of 11.9 °C and a total annual precipitation of 663 mm, on parent rock of Cretaceous sandstone. Third site was located at 1030 m asl in the Alto Duero (S3, Tardelcuende, Soria; 41°36'6"N,2°38'14"W), with a mean annual temperature of 10.7 °C and a total annual precipitation of 519 mm, on parent rock of Cenozoic sandstone. Fourth site was located at 1143 m asl in the Alto Tajo (S4, Corduente, Guadalajara; 40°49'49"N, 2° 0'27"W), with a mean annual temperature of 10.3 °C and a total annual precipitation of 490 mm, on parent rock of Triassic sandstone. Climate data were obtained from the nearest meteorological station to each site for the period 1961–2015 from AEMET (Spanish Meteorological Agency) network (see Supplementary Table 1 for further details).

Pinus pinaster is an evergreen conifer endemic to the Western Mediterranean basin inhabiting humid and sub-humid areas. It prefers acidic soils, but occasionally can grow on basic soils, with a large altitudinal distribution range from sea level to 2000 m asl (Abad Viñas et al., 2016). It is a species of major conservational and productive interest in the Iberian Peninsula that is widely used for forest restoration, wood production and resin extraction (Calama et al., 2010). *P. pinaster* secondary growth is mainly promoted by spring and early summer precipitation (Bogino and Bravo, 2008), while IADF formation is mainly linked to autumn precipitation (Vieira et al., 2010), being IADF occurring mostly in the latewood (Campelo et al., 2007; Vieira et al., 2009).

2.2. Sampling design, tree-ring width measuring and processing

We sampled twenty mature dominant or co-dominant trees (between 45 and 126 years old) at each site in February 2016. Three wood cores were taken at breast height from each stem with a 5-mm diameter increment borer. Cores were labeled and taken to the laboratory. A core per tree was reserved for microdensitometrical analysis and the other two cores were air dried and mounted on wooden supports for their processing using standard dendrochronological techniques. Cores were manually surfaced and polished with a series of progressively finer grades of sandpaper until the xylem cellular structure was clearly visible under magnification.

After visual cross-dating, tree-ring (RW), earlywood (EW) and latewood widths (LW) were measured to the nearest 0.001 mm by using a sliding stage micrometer (Velmex, Inc., USA) interfaced with a computer. Cross-dating accuracy was checked using the software COFECHA (Grissino-Mayer, 2001). Each individual raw series for measured parameter was standardized using the software ARSTAN (Cook and Holmes, 1996). Raw series were fitted to a spline function with a 50% frequency response of 32 years, which was flexible enough to reduce the non-climatic variance while preserving high-frequency climatic information (Cook and Peters, 1981), albeit long-term climatic effects are removed. EW and LW chronologies were highly correlated (reaching a maximum of $r = 0.55$; $P < .001$ in S4) reflecting common constraints and the effect of earlywood conductance on latewood growth (Pérez-de-Lis et al., 2016a; von Arx et al., 2017). Therefore, we removed the dependence of LW on EW (Babst et al., 2016), by extracting the residuals of the regression between LW and EW and dividing them by the predicted value. This procedure provided an adjusted latewood index (LW_{adj}) (Meko and Baisan, 2001) that was independent of EW chronology (Stahle et al., 2009).

2.3. Intra-annual wood density fluctuations (IADFs)

Cross-dated cores were visually analyzed under magnification for IADF identification. In accordance to their position within the tree-ring, IADFs were classified into three types (Fig. 2). IADFs type E were characterized as a latewood-like cells band within the earlywood. IADFs types L and L+ were defined as earlywood-like cells band within the latewood (L) and between latewood and earlywood of the following ring (L+) (Vieira et al., 2009). The relative proportion of IADFs occurrence was estimated as the relative frequency (F) as $F = (n_x/N) \times 100$, where n_x is the total number of cores with IADFs in the year x, and N is the total number of cores in that particular year. The IADFs type E were very scarce in almost all the sites and then were discarded for further analysis.

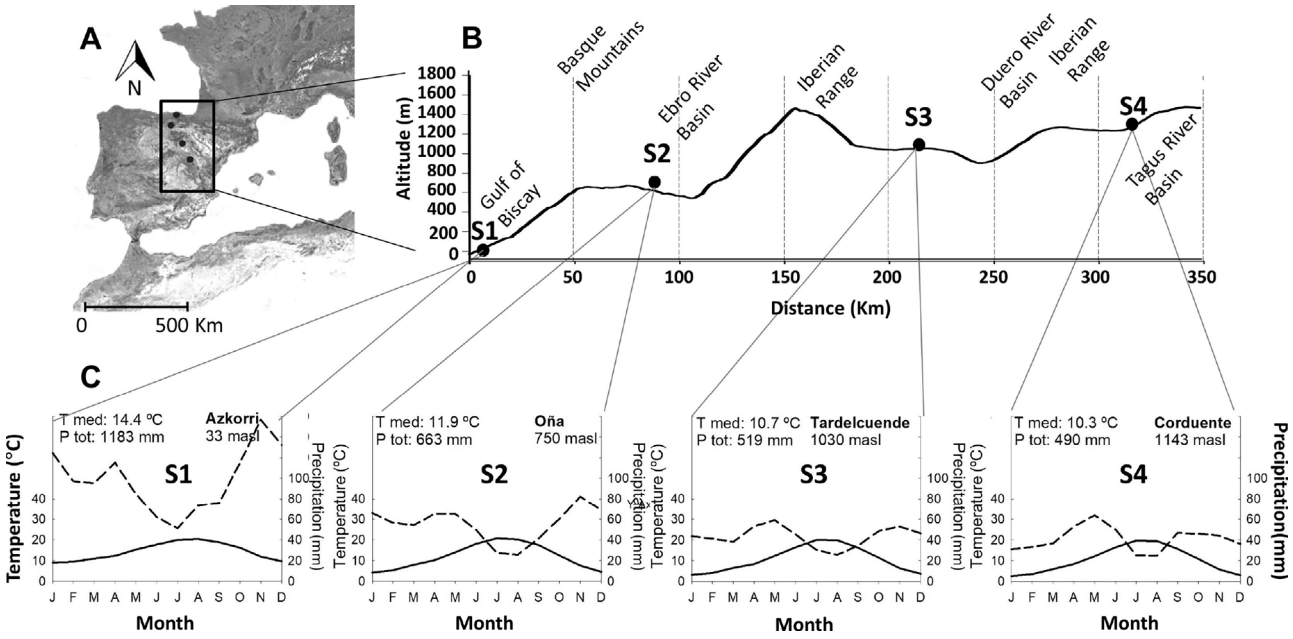

Fig. 1. Study sites location (A), altitudinal transect in Spain (B) and climodiagrams for 1961–2015 period (C). Climate data were obtained from meteorological stations within 23 km from the study sites (see Supplementary Table 1 for further details).

2.4. Microdensity profiles processing

The third core per tree was used for microdensity measurements. Cores were cut to a regular thickness of 2.3 mm using a double blade saw. Obtained samples were subjected to a resin extraction process by soaking them into pentane for 48 h before being X-rayed. Wood density was measured using indirect-reading X-ray microdensitometry (Polge, 1966), and the resulting X-rays films were scanned at 1000 dpi resolution. Images were then analyzed with the software WinDENDRO (Regent Instruments Inc., Canada). Tree-ring borders were automatically placed and subsequently manually checked for correction. All densitometric analyses were performed at INRA GENOBOIS (Orleans, France). Two density parameters were calculated at the ring level using routines written in R (R Core Team, 2016), supplied by INRA GENOBOIS: minimum ring density (D_{min}, kg dm^{-3}), and maximum ring density (D_{max}, kg dm^{-3}). Densitometric chronologies were standardized following the same protocol as for ring-width chronologies.

2.5. Statistical analysis

Patterns in xylem chronologies response were explored through a Principal Component Analysis (PCA) on the residual chronologies matrix (28 chronologies, 4 sites × 7 xylem parameters) for the common period 1966–2015 shared by all the chronologies. To settle whether the observed pattern was related to chronology parameter (seven parameters) or to site identity (four sites), a Redundancy Analysis (RDA) was performed for each constraining matrix with chronology parameter and site included as a dummy variable. A Monte Carlo permutation test

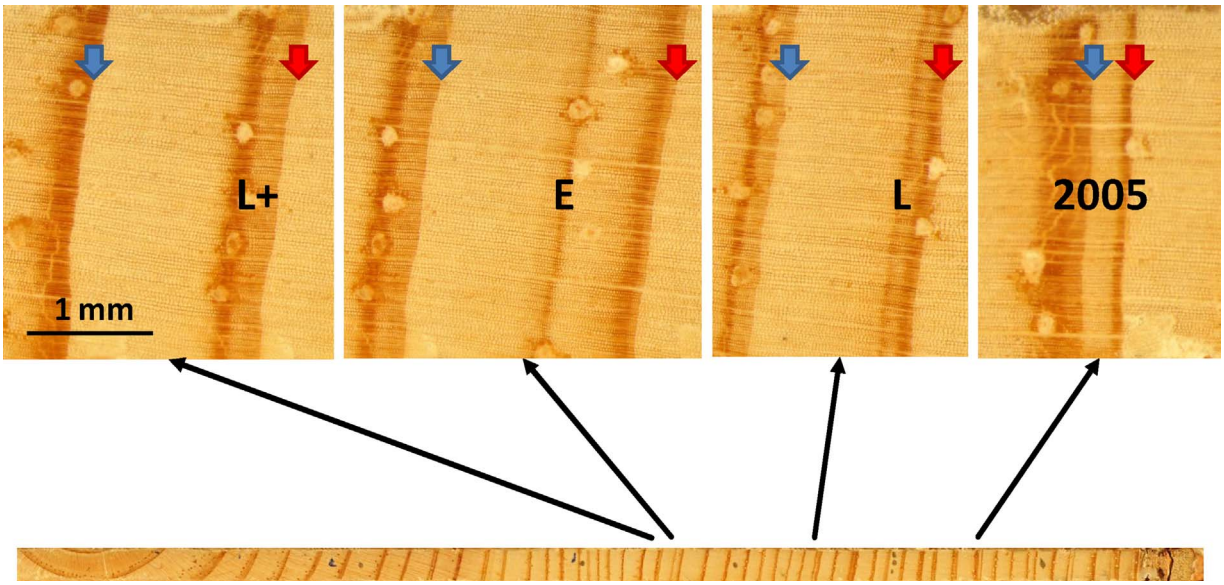

Fig. 2. *Pinus pinaster* core (below) with different IADF types and a dry year with very low growth (above). From left to right: IADF types L+, E and L, and narrow ring corresponding to the dry year 2005. Blue (left) and red (right) arrows indicate initiation and end of annual tree rings, respectively. (For interpretation of the references to colour in this figure legend, the reader is referred to the web version of this article.)

with 999 randomizations was performed to evaluate the relationship between each matrix and the chronologies (Legendre and Legendre, 2012). PCA and RDA analyses were performed with the vegan package (Oksanen et al., 2017).

We used Pearson's correlations to identify the relationship between residual RW, EW, LW_{adj}, D_{min} and D_{max} chronologies and monthly climatic factors for the common period (1961–2015) for each site, except in S1 where the sampled trees were slightly younger (1966–2015). Due to non-normality of IADF frequency chronologies, we used non-parametric Spearman correlation between climatic factors and IADF L and L + chronologies. Climatic time series (total precipitation, minimum temperature and evapotranspiration) from every meteorological station were selected for a time window comprising since September of the year before the current growth season to November of the current growth year.

We employed the Standardized Precipitation-Evaporation index (SPEI) (Vicente-Serrano et al., 2010), available at http://spei.csic.es/database.html, to evaluate the differential effect of soil water availability at different time-scales over the analyzed chronologies. SPEI incorporates precipitation and potential evapotranspiration while considering different time-scales, thus it enables to explore multiscale response of vegetation to drought (Vicente-Serrano et al., 2013). Reference evapotranspiration used to calculate the SPEI was obtained by means of the Hargreaves equation (Hargreaves and Samani, 1985) using maximum and minimum temperature and the extraterrestrial solar radiation. We calculated Pearson's correlations between RW, EW, LW_{adj}, D_{min} and D_{max} residual chronologies and SPEI index from previous September to growth year November at different timescales, with a lag ranging from one to 18 months. All statistical analyses were performed in R environment (R Core Team, 2016).

3. Results

3.1. Characterization of the xylem traits

From the 240 extracted cores, 213 from 72 *P. pinaster* trees could be cross-dated. Wood density chronologies (D_{min} and D_{max}) were based on 72 cores, one core from each sampled tree. EW, LW, IADF L and IADF L + chronologies were based on 141 cores from 72 trees, whereas RW chronologies were based on the whole data set (213 cores). RW residual chronologies showed values of mean sensitivity (ms_x) between 0.16 and 0.28, mean correlation between individuals (r_{bt}) between 0.48 and 0.68, and expressed population signals (EPS) over 0.97 in all the sites (Table 1), suggesting adequate replication and a high common signal among trees for each locality, according to Wigley et al. (1984).

RW and EW chronologies were strongly positively correlated ($r > 0.92$; $P < .001$ in all cases), a consequence of EW contributing to more than 76.64% of total RW. Both chronologies were also correlated with xylem density, positively with D_{max} and negatively with D_{min} in all the sites except in the coastal site (S1). LW_{adj} chronologies were highly and positively correlated with D_{max} in the continental sites (S3 & S4; r = 0.70–0.76; $P < .001$), whereas Atlantic sites (S1 & S2) showed non-significant correlation (r = –0.1 to 0.2; $P > .1$). Years with wider LW_{adj} showed higher IADF frequency in all sampled sites but S2. IADF L and L+ chronologies showed strong negative correlation in S1, slighter lower in S2 and were independent in the continental sites (S3 & S4) (see Supplementary Table 2 for further details). PCA analysis revealed a strong structure in residual chronologies with 88.9% of the variance explained by the first axis that had discriminated between two main groups: (1) IADF L, IADF L+ and LW_{adj} chronologies, and (2) D_{min}, D_{max} and RW-EW chronologies (Fig. 3). Partial RDA showed that chronology parameter was the most important factor explaining this structure (TVE = 91.0%; $P < .001$), whereas site identity played almost no role (TVE = 1.9%; $P > .1$).

Table 1
Summary of dendrochronological statistics for the residual chronologies for each site and parameter for the common period 1961–2015, except for S1: 1966–2015. RW, tree-ring width; EW, earlywood width; LW, latewood width; D_{min}, minimum ring density and D_{max}, maximum ring density.

Parameters	Site	Mean ± SD	ms_x	r_{bt}	EPS	SNR	AC1
RW (mm)	S1	4.32 ± 2.84	0.209	0.489	0.970	32.52	0.114
	S2	1.88 ± 1.05	0.168	0.492	0.975	39.78	−0.119
	S3	1.67 ± 1.24	0.233	0.682	0.991	115.9	−0.005
	S4	0.96 ± 0.54	0.280	0.594	0.988	83.50	−0.136
EW (mm)	S1	3.46 ± 2.35	0.422	0.406	0.949	18.47	0.022
	S2	1.49 ± 0.87	0.159	0.420	0.953	18.93	−0.039
	S3	1.28 ± 0.90	0.265	0.629	0.981	50.88	−0.064
	S4	0.74 ± 0.44	0.305	0.499	0.969	30.91	−0.082
LW (mm)	S1	0.96 ± 1.03	0.380	0.420	0.943	16.66	−0.110
	S2	0.38 ± 0.28	0.162	0.326	0.926	12.58	0.015
	S3	0.39 ± 0.46	0.255	0.446	0.962	25.00	−0.068
	S4	0.22 ± 0.19	0.263	0.246	0.910	10.12	0.011
D_{min} (kg dm^{-3})	S1	0.29 ± 0.11	0.058	0.271	0.839	5.20	−0.068
	S2	0.38 ± 0.05	0.029	0.192	0.756	3.09	0.074
	S3	0.37 ± 0.05	0.075	0.359	0.905	9.54	−0.298
	S4	0.44 ± 0.08	0.071	0.092	0.645	1.81	−0.094
D_{max} (kg dm^{-3})	S1	0.67 ± 0.25	0.073	0.193	0.544	1.19	−0.049
	S2	0.80 ± 0.11	0.039	0.124	0.586	1.41	−0.131
	S3	0.75 ± 0.12	0.057	0.453	0.930	13.24	0.048
	S4	0.65 ± 0.14	0.083	0.413	0.918	11.25	0.135

ms_x, mean sensitivity; r_{bt}, mean correlation between plants; EPS, expressed population signal; AC1, first order autocorrelation.

3.2. Climatic response of residual chronologies

Residual chronologies retrieved high correlations with climate. Correlation values were very high, especially for EW and wood density chronologies. Since EW and RW were highly correlated, only EW results with climate are presented (Fig. 4). EW responded positively to spring and early summer precipitation in May-June, albeit correlation maximum was higher earlier (May) in continental sites (S3 & S4) and later (June) in Atlantic sites (S1 & S2). December to February precipitation played a prominent role in continental sites, but was irrelevant in the Atlantic sites, which showed a small positive response to previous year September–October rainfall. Minimum temperatures during winter also exerted positive effects in cooler continental sites (S3 & S4), but only a minor effect in the site S2 with more oceanic influence. Results of the correlation between SPEI and EW revealed a high correlation of EW with the hydric balance (Fig. 5). The intensity of SPEI correlation increased from the coastal to the continental sites, from a minimum of 22.1% of explained variance in S1 to a maximum of 57.7% in S3. The timing of the maximum correlation was earlier and lasted longer in the continental sites S3 & S4 (June, 9 mo), and occurred later in the year and had a shorter temporal lag in the oceanic sites (S1: August, 6 mo; S2: August, 4 mo).

LW residual chronologies were moderately but significantly correlated with EW one (r = 0.40–0.55; $P < .05$) in all sites except S2 (see Supplementary Table 2 for further details), where it showed a non-significant correlation (r = –0.21; $P > .1$). Residual chronologies of LW_{adj} showed a positive response to rainfall during latewood formation in July–September, with site-related differences in the timing and lag (Fig. 4). The maximum correlation had a shorter temporal lag and occurred later in the year in the oceanic sites (August in S2, September in S1). It also responded to precipitation in two periods before secondary growth initiation, with positive responses to December to January precipitation in all but the coastal site, whereas precipitation in October, at the end of the previous growing season, had a negative effect in both continental sites (S3 & S4). SPEI explained a significant proportion of LW_{adj} variability (Fig. 5), ranging from 21.1% in S2 to 30.1% in S4. The timing of LW_{adj} maximum correlation, at the end of summer

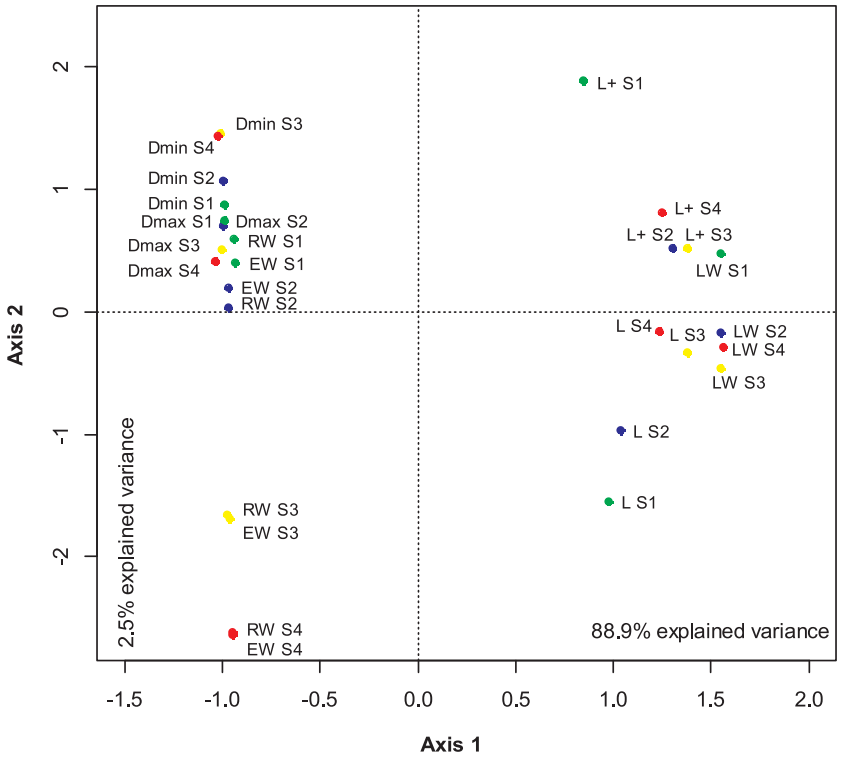

Fig. 3. Principal Component Analysis (PCA) on the residual chronologies of *Pinus pinaster* for the common period 1966–2015. *Dmin:* Minimum density; *Dmax:* Maximum density; *EW:* Earlywood width; *L:* L IADF; *L+:* L+ IADF; *LW:* Adjusted latewood width; *RW:* Ring width. Colors correspond to sites, green for S1, blue for S2, yellow for S3 and red for S4. (For interpretation of the references to colour in this figure legend, the reader is referred to the web version of this article.)

or in early autumn, and its lag, showed a great coordination with EW-SPEI relationships, in all sites but S2. In S1, EW maximum correlation occurred in August, whereas LW_{adj} correlation peaked in October with two months' lag. EW climatic signal peaked in the continental sites (S3 & S4) in June, and LW_{adj} correlation had its maxima in September with a 3-month lag (from July to September).

D_{min} responded to conditions during spring (Fig. 6), with higher spring precipitation resulting in reduced D_{min} in all but the coastal site S1, and this effect extending to winter in the continental sites S3 & S4. In contrast, early-summer precipitation in June–July (Fig. 6) had a positive effect in the coastal site S1. Minimum temperature in January–February also showed a negative effect in the continental sites (S3 & S4). SPEI signal (Fig. 5) matched the observed monthly climatic effect, revealing a negative effect of wet springs on D_{min} ($r^2 = 0.473$, $P < .0001$ in S2; $r^2 = 0.474$, $P < .0001$ in S3; $r^2 = 0.246$, $P < .001$ in S4), with both continental sites showing longer lags that included winter. In contrast, SPEI had a poor effect for the coastal site ($r^2 = 0.162$; $P = .004$ in S1), with higher D_{min} associated to wet June–July months.

Residual chronologies of D_{max} (Fig. 6) reflected the positive effect of

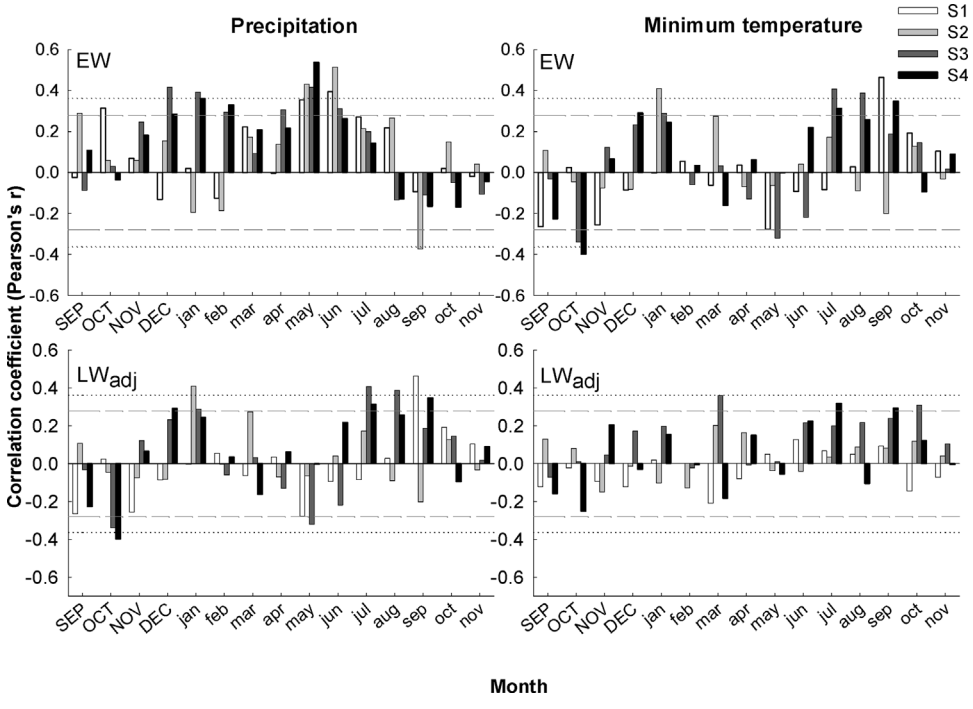

Fig. 4. Correlations (Pearson's coefficient) between earlywood (EW) and latewood adjusted (LW_{adj}) with total precipitation and minimum temperature for the period 1961–2015, except for S1: 1966–2015. Correlations were calculated from September of previous year (uppercase letters) to November of current growth year (lowercase letters). Dashed lines indicated $P < .05$ and dotted lines indicate $P < .01$. Bars colors indicate the four sampled sites (S1, white; S2, grey; S3, dark grey and S4, black).

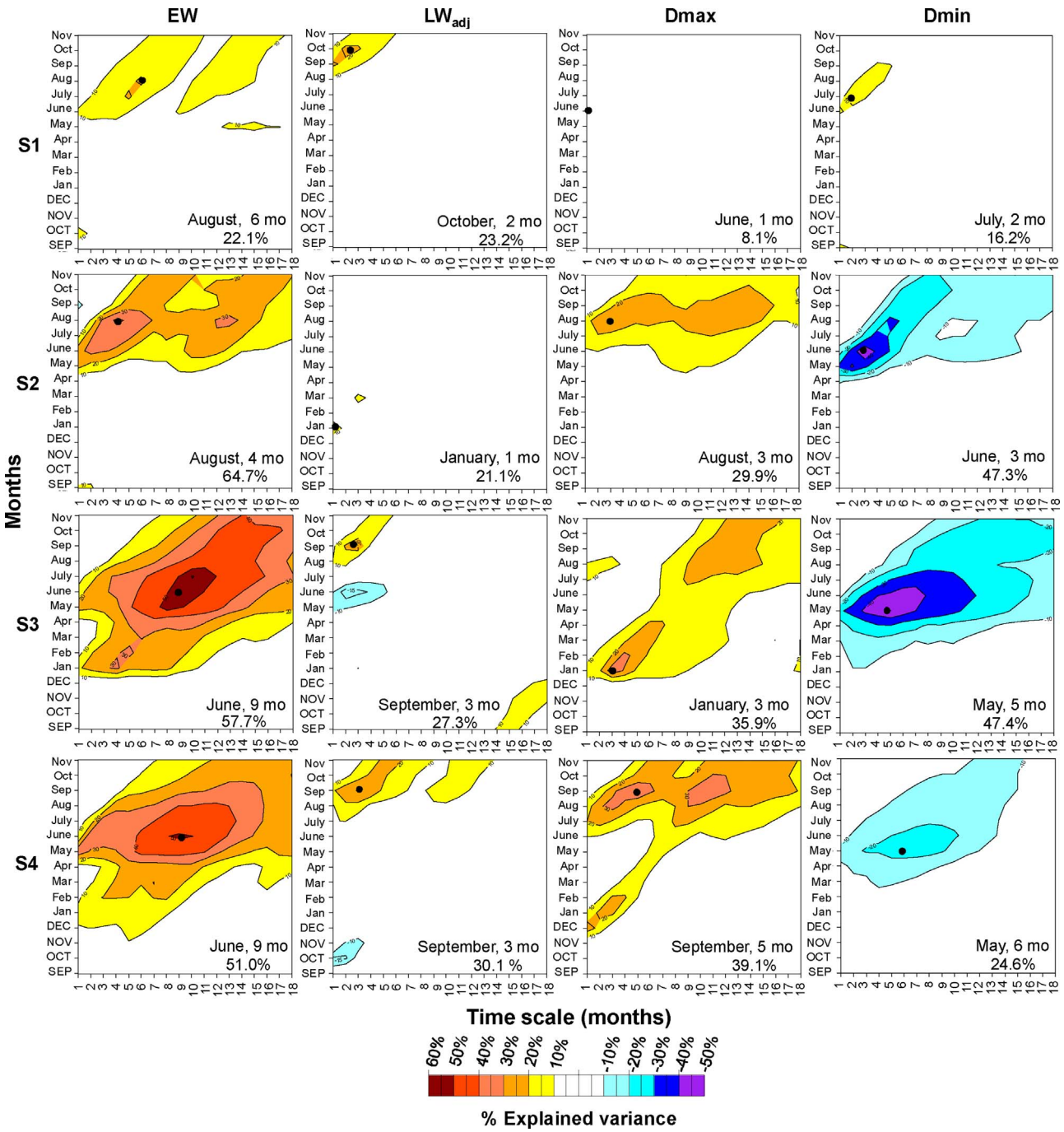

Fig. 5. Percentage of the variance of Earlywood width (EW), adjusted latewood width (LW_{adj}), minimum ring density (Dmin) and maximum ring density (Dmax) chronologies explained by monthly Standardized Precipitation–Evaporation index (SPEI) series at different time scales for the period 1961–2015, except for S1: 1966–2015. The correlations were calculated from September of the previous year (uppercase letters) to November of the current year (lowercase letters) of tree ring formation. Inserts in the plots represent the month and temporal lag in which maximum appears and percentage of explained variance. Black dots indicate the maximum signal occurrence. Percentage of variance is calculated as the variance explained by the coefficient of determination (R^2), but retaining the sign of r to evaluate the direction of the effect. This parameter improves the visibility of optimal statistical relationships between growth and SPEI.

cumulative June to August precipitation in the inland sites S2, S3 & S4. Interestingly, in the more continental sites S3 & S4, December–January precipitation had an even stronger positive value and precipitation in October, at the end of the previous growing season, showed a negative effect. January to March minimum temperature had a reduced positive effect in the inland sites S2, S3 & S4. SPEI explanatory power (Fig. 5) grew with increasing continentality ($r^2 = 0.081$, $P = .045$ in S1; $r^2 = 0.299$, $P < .0001$ in S2; $r^2 = 0.359$, $P < .0001$ in S3; $r^2 = 0.391$, $P < .0001$ in S4). Maximum correlation timing shifted from maxima in June (1 mo) for the coastal site S1, August (3 mo) for S2, to two peaks in continental sites, one in winter (January, 3 mo) that was the maxima in S3, and another at the end of summer (September, 5 mo), that was the highest in S4.

3.3. Climatic control on IADF formation

IADFs were very common in the latewood, ranging between 21–22% in the continental sites S3 & S4, to 51% in the coastal site S1. However, IADF E occurred only in three rings in the coastal site, and none in the other sites. No significant temporal trend was found in total

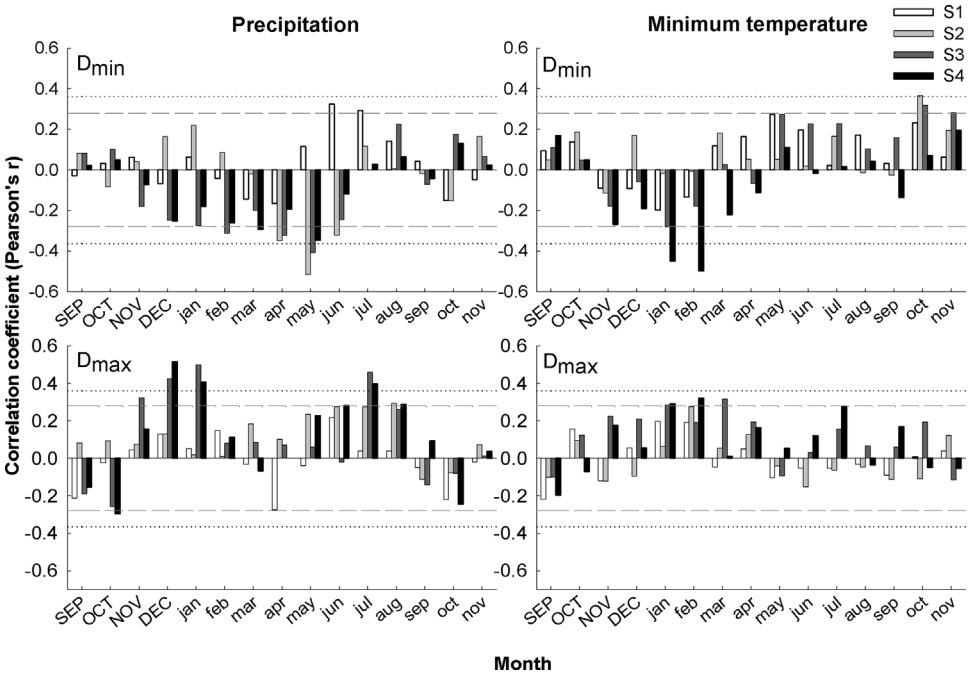

Fig. 6. Correlations (Pearson's coefficient) between minimum density (D_{min}) and maximum density (D_{max}) with total precipitation and minimum temperature for the period 1961–2015, with the exception of 1966–2015 for S1. Correlations were calculated from September of previous year (uppercase letters) to November of current year (lowercase letters). Dashed lines indicated $P < .05$ and dotted lines indicate $P < .01$. Bars colors indicate the four samples sites (S1, white; S2, grey; S3, dark grey and S4, black).

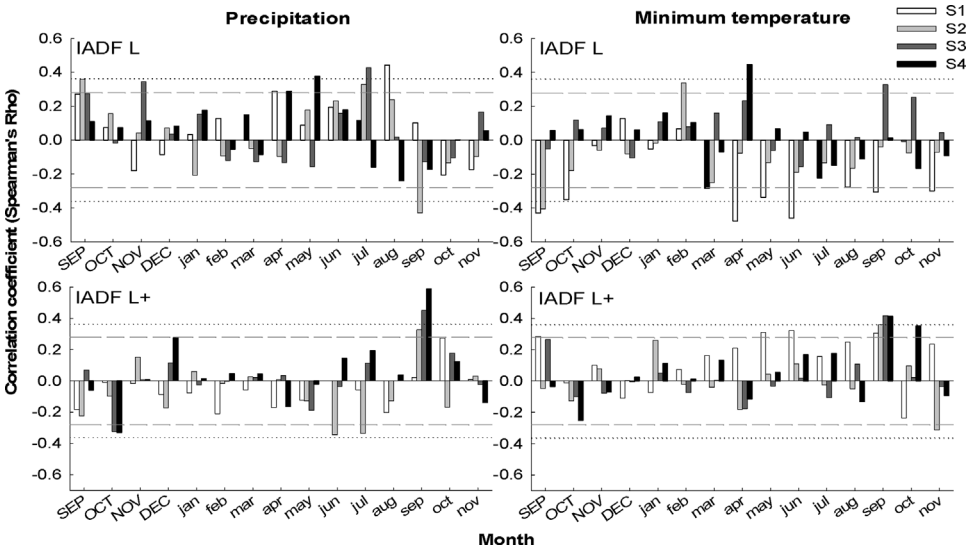

Fig. 7. Non-parametric correlations (Spearman's Rho) between IADF types L and L+ with total precipitation and minimum temperature for the period 1961–2015, with the exception of 1966–2015 for S1. Correlations were calculated from September of previous year (uppercase letters) to November of current year (lowercase letters). Dashed lines indicated $P < .05$ and dotted lines indicate $P < .01$. Bars colors indicate the four samples sites (S1, white; S2, grey; S3, dark grey and S4, black).

IADF frequency in any site, although in the coastal site IADF L declined ($r = –0.53$, $P < .001$) whereas IADF L+ increased ($r = 0.36$, $P = .009$). IADF L were more frequent than L+ in S2 and S3, but both IADF types showed similar frequencies in S1 and S4. Spearman's correlation revealed contrasting responses to climatic factors between both IADF types in the latewood (Fig. 7). IADF L frequency increased with higher than average rainfall during summer arrest, July in S2 and S3 and August in S1. By contrast, IADF L+ occurrence was associated to wet and warm early autumn conditions.

4. Discussion

The use of a multiproxy approach along a climatic gradient allowed unveiling robust links between climate and *Pinus pinaster* xylem characteristics. Water availability had a dramatic impact on all analyzed wood traits. The timing of the climatic factors constraining cambium activity varied along the climatic gradient. Nevertheless, the identity of the analyzed traits outperformed geographic location in determining limiting climatic conditions. Latewood growth and IADF frequency responded to climatic factors occurring in a different temporal domain than earlywood width and microdensity.

Earlywood formation initiates after a minimum temperature threshold for cambial activity is reached (Kulmala et al., 2017; Rossi et al., 2008; Vieira et al., 2014; but see Ren et al., 2015), and extends in Mediterranean areas until spring-summer drought depletes soil moisture, leading to cambial cells division halt (Camarero et al., 2010). The span of this period varies considerably along the wide range of environmental conditions inhabited by *P. pinaster*. This variability is highlighted by the contrasting intensity and timing of the earlywood climatic signals along the continentality-aridity gradient. Drier continental Mediterranean sites experienced water limitation earlier, more intensely and for longer time periods than humid and warm Atlantic sites. In fact, water limitation was so high that earlywood growth in continental sites depended on autumn-winter precipitation that recharges soil water, whereas earlywood growth in Atlantic sites only responded to variability of spring-summer precipitation. An earlier onset of cambial activity in *P. pinaster* under dry and warm conditions might prolong the length of xylogenesis period before summer drought

(Campelo et al., 2007; Vieira et al., 2010, 2009), favoring higher tracheid production (Lupi et al., 2010). However, in dry and cool continental sites, late-winter temperatures may represent a strong thermal limitation to earlier initiation of cambial activity.

Latewood contributed significantly to total ring width, comprising 24% of total ring. Since latewood production was dependent on earlywood production, removing EW signal in LW resulted in an enhanced LW climatic signal. The transition between earlywood and latewood can be controlled by different factors, including soil moisture (Domec and Gartner, 2002), thus a decrease of water availability along the gradient would induce earlier LW initiation in drier sites. Sooner early-latewood transition in drier sites was supported by an earlier SPEI signal in LW_{adj} in dry continental sites. Overall, *P. pinaster* growth responded to water availability along the whole growing season, both early and latewood growth being constrained by water availability. The timing of SPEI signals in EW and LW_{adj} chronologies undoubtedly reflects the continuous water limitation of secondary growth. For example, maximal SPEI signal for earlywood growth in the Cantabrian coast occurred in August with a six months' lag (from March to August), whereas latewood responded to the immediate period, October with a two months' lag (from September to October). Arrest of *P. pinaster* xylogenesis has been related to temperature, with longer growing seasons occurring under warmer conditions (Campelo et al., 2013; Vieira et al., 2014). Temperature limitation for latewood growth in colder sites is reflected by the later LW_{adj} climatic signals in coastal sites and the limiting effect of autumn minimal temperatures in more continental sites.

Unpredictable rainfall patterns in Mediterranean environments result in a high frequency of the activation-reactivation cycles in cambial activity during the growing season (Campelo et al., 2007; Olano et al., 2015; Zalloni et al., 2016). These changes can be recognized through the identification of IADFs, which are extremely common in *P. pinaster* during latewood formation under both Atlantic and Mediterranean climates (Battipaglia et al., 2016; Bogino and Bravo, 2009; Campelo et al., 2015; De Micco et al., 2007; Rozas et al., 2011; Vieira et al., 2010, 2009). Latewood IADFs formation in Mediterranean conifers is driven by increased soil water availability during the late growing season, which is reflected in larger tracheid lumens (Pacheco et al., 2016). Also, a modelling approach proved that water availability is the key driver of wood density variation and IADF formation in the latewood of *P. pinaster* (Wilkinson et al., 2016). In our case, the formation of IADF types L or L+ depended on the timing where the climatic event occurred. Higher rainfall during the early-latewood transition period was strongly correlated with IADF L formation in three out of four sites, whereas IADF L+ tended to occur under warm and wet conditions in September, or after October rainfall in the coast, near the end of latewood formation. Despite the different timing of the climatic signal, both IADF types in the latewood are a consequence of the same physiological process, i.e. increased water availability during latewood cell expansion, that leads to enhanced cell turgor pressure and larger tracheid lumens (Carvalho et al., 2015; Oberhuber et al., 2014; Vieira et al., 2015). If this phenomenon occurs near the onset of latewood formation, IADFs type L is formed, whereas if it takes place near the end of latewood formation, IADFs type L+ appears. The preconditioning effects of high temperature showed to be opposite for L and L+ IADFs formation in coastal stands, being negative in April-June for L frequency and positive in May–June for L+ frequency. In inner stands, however, both L and L + frequencies showed to be positively related to elevated temperatures, in April for L formation and in September–October for L+ formation. This result is similar to those observed for *P. pinaster* in NW Spain (Rozas et al., 2011), and can be attributed to the intensification of cambial activity under warm conditions in key phases of the xylogenetic cycle. In general, IADFs formation in Mediterranean pines shows positive relations with temperature (Zalloni et al., 2016), which induces an enlargement of the growing season and a higher frequency of IADFs (Campelo et al., 2015).

Wood density integrates multiple anatomical parameters, e.g. tracheid lumen to wall ratio, secondary wall lignification, and proportion of parenchyma in the xylem, thus resulting in a good proxy for xylem anatomy. To date, most studies exploring inter-annual variability in xylem density have focused on maximum density. This may reflect the strong functional link between higher summer temperatures and longer and more intense cell-wall thickening in temperature-limited temperate and boreal environments (Briffa et al., 1998; Büntgen et al., 2010; Vaganov et al., 1999). Thus, maximum density retrieves a strong late summer temperature signature (Kirdyanov et al., 2003, 2007; Büntgen et al., 2010). Nevertheless, it is not evident whether the same processes may act in Mediterranean environments where growth is mostly controlled by water availability. Higher water availability during latewood formation may impact directly tracheid maturation processes and increase cell wall thickness (Olano et al., 2012, 2014), with this signal being stronger and responding to longer temporal lags in more water-limited continental sites. In contrast, the impact of winter rainfall on latewood formation in the two Mediterranean-continental sites would be related to indirect mechanisms. Warm and wet winters would favor photosynthetic activity leading to increased carbon reserves. Higher resource accumulation may directly provide additional resources to invest in photosynthetic tissue leading to more carbon gain, directly in the construction of the costly latewood cells, or in the gain of earlywood conductive tissue (DeSoto et al., 2016; Kulmala et al., 2017; Vicente-Serrano et al., 2016; von Arx et al., *in review*). Our results add to the few published microdensitometrical analyses in Mediterranean conifers and point to a complex link between maximum density and water availability at distinct periods (Camarero et al., 2014; Besson et al., 2016).

The strong spring precipitation signal found in D_{min} confirms previous research in drought constrained environments (Camarero et al., 2014; Cleaveland, 1986). Higher water availability during earlywood tracheid expansion would result in wider tracheids (Oberhuber et al., 2014) with higher lumen to wall ratio and potentially also higher parenchyma proportion (Olano et al., 2013a), altogether decreasing wood density and promoting its conductive efficiency. In this sense, the negative correlation between EW and D_{min} in our data, could respond to a common but opposite climate forcing, but it may also be revealing an additional positive feed-back of higher conductivity on xylem growth (Olano et al., 2013b; Pérez-de-Lis et al., 2017).

Regardless of the regional variation in limiting climatic conditions, the variability associated to xylem trait identity outperformed site-related environmental shifts along the studied gradient. All parameters responded to water availability, but there was a divide of earlywood growth, ring width and densitometric measurements against latewood growth and IADF formation, which indicates that the climatic signals controlling two groups of parameters are occurring at different time domains. Latewood growth and IADF formation respond to events occurring in late summer and early autumn, whereas earlywood and densitometry signals occur mostly prior to latewood formation. The strong climatic signals revealed by our results highlight the considerable potential of multi-proxy tree-ring approaches to reconstruct climate variability in Mediterranean climates.

A high plasticity in cambial activity and xylogenesis is one of the most relevant factors to overcome the unpredictable climatic conditions imposed by Mediterranean climate (Camarero et al., 2010; Cherubini et al., 2003; Gutiérrez et al., 2011). The ability to modify the onset and the rate of xylogenesis and to arrest and resume cambial activity, exploiting favorable climatic windows, allow Mediterranean plants to maintain secondary growth activity under wide climatic envelopes (Arzac et al., 2016; Camarero et al., 2010; Olano et al., 2015). This plasticity may explain why an increase in climatic suitability has been predicted for *P. pinaster* under future climate scenarios (Lloret et al., 2013). Nevertheless, the pervasive effect of water availability in all analyzed traits indicates that reduced precipitation and increased evapotranspiration, as predicted by climate change models for the Mediterranean region (Giorgi and Lionello, 2008), will impact negatively *P.*

pinaster secondary growth along its whole distribution range. Moreover, the limited genetic variation in the resistance to embolism along its distribution range (Corcuera et al., 2012; Lamy et al., 2014) indicates the existence of a net threshold in its potential drought tolerance and susceptibility to future increased drought in its arid range edge.

Acknowledgements

We are indebted to INRA GENOBOIS Wood analysis technical platform (Orleans, France) for technical support and to Frédéric Millier for X-ray films preparation. This study was supported by the Transnational Access to Research Infrastructures activity in the 7th Framework Program of the EC under the Trees4Future project (no. 284181). A. Arzac contract was supported by the Russian Ministry of Education, PostDoctoral Program of Project "5-100" [Grant № M 2.2.3]. A previous version was revised by A. Kirdyanov and A.I. García-Cervigón.

Appendix A. Supplementary data

Supplementary material related to this article can be found, in the online version, at doi:https://doi.org/10.1016/j.agrformet.2017.12.257

References

Abad Viñas, R., Caudullo, G., Oliveira, S., de Rigo, D., 2016. In: San-Miguel-Ayanz, J., de Riego, D., Caudullo, G., Houston Durant, T., Mauri, A. (Eds.), *Pinus pinaster* in Europe: Distribution, Habitat, Usage and Threats. I. European Atlas of Forest Tree Species, Luxenburg, pp. 126–127.

Antonucci, S., Rossi, S., Deslauriers, A., Morin, H., Lombardi, F., Marchetti, M., Tognetti, R., 2017. Large-scale estimation of xylem phenology in black spruce through remote sensing. Agric. For. Meteorol. 233, 92–100. http://dx.doi.org/10.1016/j.agrformet.2016.11.011.

Arzac, A., García-Cervigón, A.I., Vicente-Serrano, S.M., Loidi, J., Olano, J.M., 2016. Phenological shifts in climatic response of secondary growth allow *Juniperus sabina* L. to cope with altitudinal and temporal climate variability. Agric. For. Meteorol. 217, 35–45. http://dx.doi.org/10.1016/j.agrformet.2015.11.011.

Babst, F., Wright, W.E., Szejner, P., Wells, L., Belmecheri, S., Monson, R.K., 2016. Blue intensity parameters derived from Ponderosa pine tree rings characterize intra-annual density fluctuations and reveal seasonally divergent water limitations. Trees 30, 1403–1415. http://dx.doi.org/10.1007/s00468-016-1377-6.

Battipaglia, G., Campelo, F., Vieira, J., Grabner, M., De Micco, V., Nabais, C., Cherubini, P., Carrer, M., Bräuning, A., Čufar, K., Di Filippo, A., García-González, I., Koprowski, M., Klisz, M., Kirdyanov, A.V., Zafirov, N., de Luis, M., 2016. Structure and function of intra–annual density fluctuations: mind the gaps. Front. Plant Sci. 7, 595. http://dx.doi.org/10.3389/fpls.2016.00595.

Besson, C.K., Lousada, J.P., Gaspar, M.M., Correia, I.E., David, T.S., Soares, P.M., Cardoso, R.M., Russo, A.C., Varino, F., Mériaux, C., Trigo, R.M., Gouveira, C.M., 2016. The effects of recent minimum temperature and water deficit increases on *Pinus pinaster* radial growth and wood density in Southern Portugal. Front. Plant Sci. 7, 1170. http://dx.doi.org/10.3389/fpls.2016.01170.

Bogino, S., Bravo, F., 2008. Growth response of Pinus pinaster Ait. to climatic variables in central Spanish forests. Ann. For. Sci 65, 506. http://dx.doi.org/10.1051/forest:2008025.

Bogino, S., Bravo, F., 2009. Climate and intraannual density fluctuations in *Pinus pinaster* subsp. *mesogeensis* in Spanish woodlands. Can. J. For. Res. 39, 1557–1565. http://dx.doi.org/10.1139/X09-074.

Briffa, K.R., Schweingruber, F.H., Jones, P.D., Osborn, T.J., Shiyatov, S.G., Vaganov, E.A., 1998. Reduced sensitivity of recent tree-growth to temperature at high northern latitudes. Nature 391, 678–682. http://dx.doi.org/10.1038/35596.

Büntgen, U., Frank, D., Trouet, V., Esper, J., 2010. Diverse climate sensitivity of Mediterranean tree-ring width and density. Trees. 24, 261–273. http://dx.doi.org/10.1007/s00468-009-0396-y.

Calama, R., Tomé, M., Sánchez-González, M., Miina, J., Spanos, K., Palahí, M., 2010. Modelling non-wood forest products in Europe: a review. For. Syst. 19, 69–85. http://dx.doi.org/10.5424/fs/201019S-9324.

Camarero, J.J., Olano, J.M., Parras, A., 2010. Plastic bimodal xylogenesis in conifers from continental Mediterranean climates. New Phytol. 185, 471–480. http://dx.doi.org/10.1111/j.1469-8137.2009.03073.x.

Camarero, J.J., Rozas, V., Olano, J.M., 2014. Minimum wood density of *Juniperus thurifera* is a robust proxy of spring water availability in a continental Mediterranean climate. J. Biogeogr. 41, 1105–1114. http://dx.doi.org/10.1111/jbi.12271.

Campelo, F., Nabais, C., Freitas, H., Gutiérrez, E., 2007. Climatic significance of tree-ring width and intra-annual density fluctuations in *Pinus pinea* from a dry Mediterranean area in Portugal. Ann. For. Sci. 64, 229–238. http://dx.doi.org/10.1051/forest2006107.

Campelo, F., Vieira, J., Battipaglia, G., de Luis, M., Nabais, C., Freitas, H., Cherubini, P., 2015. Which matters most for the formation of intra-annual density fluctuations in *Pinus pinaster*: age or size? Trees 29, 237–245. http://dx.doi.org/10.1007/s00468-014-1108-9.

Campelo, F., Vieira, J., Nabais, C., 2013. Tree-ring growth and intra-annual density fluctuations of *Pinus pinaster* responses to climate: does size matter? Trees 27, 763–772. http://dx.doi.org/10.1007/s00468-012-0831-3.

Carvalho, A., Nabais, C., Vieira, J., Rossi, S., Campelo, F., 2015. Plastic response of tracheids in *Pinus pinaster* in a water-limited environment: adjusting lumen size instead of wall thickness. PLoS One 10. http://dx.doi.org/10.1371/journal.pone.0136305.

Chave, J., Coomes, D., Jansen, S., Lewis, S.L., Swenson, N.G., Zanne, A.E., 2009. Towards a worldwide wood economics spectrum. Ecol. Lett. 12, 351–366. http://dx.doi.org/10.1111/j.1461-0248.2009.01285.x.

Cherubini, P., Gartner, B.L., Tognetti, R., Bräker, O.U., Schoch, W., Innes, J.L., 2003. Identification, measurement and interpretation of tree rings in woody species from Mediterranean climates. Biol. Rev. 78, 119–148. http://dx.doi.org/10.1017/S1464793102006000.

Cleaveland, M.K., 1986. Climatic response of densitometric properties in semiarid site tree rings. Tree—Ring Bull. 46, 13–29.

Cook, E.R., Holmes, R., 1996. Guide for computer program ARSTAN. I. In: Grissino-Mayer, H.D., Holmes, R.L., Fritts, H.C. (Eds.), The Internarional Tree-Ring Data Bank Program Library Version 2.0 User's Manual. Laboratoty of Tree-Ring Reseach, Universisty of Arizona, Tucson, USA, pp. 75–87.

Cook, E.R., Peters, K., 1981. The smoothing spline: a new approach to standardizing forest interior tree-ring width series for dendroclimatic studies. Tree—Ring Bull. 41, 45–53.

Corcuera, L., Gil-Pelegrín, E., Notivol, E., 2012. Differences in hydraulic architecture between mesic and xeric *Pinus pinaster* populations at the seedling stage. Tree Physiol. 32, 1442–1457. http://dx.doi.org/10.1093/treephys/tps103.

De Micco, V., Saurer, M., Aronne, G., Tognetti, R., Cherubini, P., 2007. Variations of wood anatomy and δ13C within-tree rings of coastal *Pinus pinaster* showing intra-annual density fluctuations. IAWA J. 28, 61–74. http://dx.doi.org/10.1163/22941932-20160132.

DeSoto, L., Olano, J.M., Rozas, V., 2016. Secondary growth and carbohydrate storage patterns differ between sexes in Juniperus thurifera. Front. Plant Sci. 7, 723. http://dx.doi.org/10.3389/fpls.2016.00723.

Domec, J.-C., Gartner, B.L., 2002. How do water transport and water storage differ in coniferous earlywood and latewood? J. Exp. Bot. 53, 2369–2379. http://dx.doi.org/10.1093/jxb/erf100.

Fonti, P., Von Arx, G., García-González, I., Eilmann, B., Sass-Klaassen, U., Gärtner, H., Eckstein, D., 2010. Studying global change through investigation of the plastic responses of xylem anatomy in tree rings. New Phytol. 185, 42–53. http://dx.doi.org/10.1111/j.1469-8137.2009.03030.x.

Frank, D., Reichstein, M., Bahn, M., Thonicke, K., Frank, D., Mahecha, M.D., Smith, P., van der Velde, M., Vicca, S., Babst, F., Beer, C., Buchmann, N., Canadell, J.G., Ciais, P., Cramer, W., Ibrom, A., Miglietta, F., Poulter, B., Rammig, A., Seneviratne, S.I., Walz, A., Wattenbach, M., Zavala, M.A., Zscheischler, J., 2015. Effects of climate extremes on the terrestrial carbon cycle: concepts, processes and potential future impacts. Glob. Change Biol. 21, 2861–2880. http://dx.doi.org/10.1111/gcb.12916.

Fritts, H.C., 1976. Tree Ring and Climate. Academic Press, London.

Giorgi, F., Lionello, P., 2008. Climate change projections for the Mediterranean region. Glob. Planet. Change 63, 90–104. http://dx.doi.org/10.1016/j.gloplacha.2007.09.005.

Granda, E., Camarero, J.J., Gimeno, T.E., Martínez-Fernández, J., Valladares, F., 2013. Intensity and timing of warming and drought differentially affect growth patterns of co-occurring Mediterranean tree species. Eur. J. For. Res. 132, 469–480. http://dx.doi.org/10.1007/s10342-013-0687-0.

Grissino-Mayer, H.D., 2001. Evaluating crossdating accuracy: a manual and tutorial for the computer program COFECHA. Tree—Ring Res. 57, 205–221.

Gutiérrez, E., Campelo, F., Camarero, J.J., Ribas, M., Muntán, E., Nabais, C., Freitas, H., 2011. Climate controls act at different scales on the seasonal pattern of *Quercus ilex* L. stem radial increments in NE Spain. Trees 25, 637–646. http://dx.doi.org/10.1007/s00468-011-0540-3.

Hargreaves, G.L., Samani, Z.A., 1985. Reference crop evapotranspiration from temperature. Appl. Eng. Agric. 1, 96–99.

IPCC, 2014. Climate Change 2014: Synthesis Report. Contribution of Working Groups I, II and III to the Fifth Assessment Report of the Intergovernmental Panel on Climate Change. Core Writing Teamhttp://dx.doi.org/10.1017/CBO9781107415324.004. R. K. Pachauri and L.A. Meyer.

Kirdyanov, A.V., Vaganov, E.A., Hughes, M.K., 2007. Separating the climatic signal from tree-ring width and maximum latewood density records. Trees 21, 37–44. http://dx.doi.org/10.1007/s00468-006-0094-y.

Kirdyanov, A., Hughes, M., Vaganov, E.A., Schweingruber, F., Silkin, P., 2003. The importance of early summer temperature and date of snow melt for tree growth in the Siberian Subarctic. Trees 17, 61–69. http://dx.doi.org/10.1007/s00468-002-0209-z.

Kulmala, L., Read, J., Nöjd, P., Rathgeber, C.B.K., Cuny, H.E., Hollmén, J., Mäkinen, H., 2017. Identifying the main drivers for the production and maturation of Scots pine tracheids along a temperature gradient. Agric. For. Meteorol. 232, 210–224. http://dx.doi.org/10.1016/j.agrformet.2016.08.012.

Lal, R., 2008. Sequestration of atmospheric CO2 in global carbon pools. Energy Environ. Sci. 1, 86–100. http://dx.doi.org/10.1039/b809492f.

Lamy, J.-B., Delzon, S., Bouche, P.S., Alia, R., Vendramin, G.G., Cochard, H., Plomion, C., 2014. Limited genetic variability and phenotypic plasticity detected for cavitation resistance in a Mediterranean pine. New Phytol. 201, 874–886. http://dx.doi.org/10.1111/nph.12556.

Legendre, P., Legendre, L., 2012. Numerical Ecology. Elsevierm, Quebec.

Lloret, F., Martinez-Vilalta, J., Serra-Diaz, J.M., Ninyerola, M., 2013. Relationship

between projected changes in future climatic suitability and demographic and functional traits of forest tree species in Spain. Clim. Change 120, 449–462. http://dx.doi.org/10.1007/s10584-013-0820-6.

Lupi, C., Morin, H., Deslauriers, A., Rossi, S., 2010. Xylem phenology and wood production: resolving the chicken-or-egg dilemma. Plant Cell Environ. 33, 1721–1730. http://dx.doi.org/10.1111/j.1365-3040.2010.02176.x.

Meko, D.M., Baisan, C.H., 2001. Pilot study of latewood-width of conifers as an indicator of variability of summer rainfall in the North American monsoonregion. Int. J. Climatol. 21, 697–708. http://dx.doi.org/10.1002/joc.646.

Oberhuber, W., Gruber, A., Kofler, W., Swidrak, I., 2014. Radial stem growth in response to microclimate and soil moisture in a drought-prone mixed coniferous forest at an inner Alpine site. Eur. J. For. Res. 133, 467–479. http://dx.doi.org/10.1007/s10342-013-0777-z.

Oksanen, J., Blanchet, F.G., Friendly, M., Kindt, R., Legendre, P., McGlinn, D., Minchin, P.R., O'Hara, R.B., Simpson, G.L., Solymos, P., Stevens, M.H.H., Szoecs, E., Wagner, H., 2017. Vegan: Community Ecology Package. R Package Version 2.4-2. https://CRAN.R-project.org/pa.

Olano, J.M., Almería, I., Eugenio, M., von Arx, G., 2013b. Under pressure: how a Mediterranean high-mountain forb coordinates growth and hydraulic xylem anatomy in response to temperature and water constraints. Funct. Ecol. 27, 1295–1303. http://dx.doi.org/10.1111/1365-2435.12144.

Olano, J.M., Arzac, A., García-Cervigón, A.I., von Arx, G., Rozas, V., 2013a. New star on the stage: amount of ray parenchyma in tree rings shows a link to climate. New Phytol. 198, 486–495. http://dx.doi.org/10.1111/nph.12113.

Olano, J.M., Eugenio, M., García-Cervigón, A.I., Folch, M., Rozas, V., 2012. Quantitative tracheid anatomy reveals a complex environmental control of wood structure in continental Mediterranean climate. Int. J. Plant Sci. 173, 137–149. http://dx.doi.org/10.1086/663165.

Olano, J.M., García-Cervigón, A.I., Arzac, A., Rozas, V., 2015. Intra-annual wood density fluctuations and tree-ring width pattern are sex- and site-dependent in the dioecious conifer *Juniperus thurifera* L. Trees 29, 1341–1353. http://dx.doi.org/10.1007/s00468-015-1212-5.

Olano, J.M., Linares, J.C., García-Cervigón, A.I., Arzac, A., Delgado, A., Rozas, V., 2014. Drought-induced increase in water-use efficiency reduces secondary tree growth and tracheid wall thickness in a Mediterranean conifer. Oecologia 176, 273–283. http://dx.doi.org/10.1007/s00442-014-2989-4.

Pacheco, A., Camarero, J.J., Carrer, M., 2016. Linking wood anatomy and xylogenesis allows pinpointing of climate and drought influences on growth of coexisting conifers in continental Mediterranean climate. Tree Physiol. 36, 502–512. http://dx.doi.org/10.1093/treephys/tpv125.

Pérez-de-Lis, G., García-González, I., Rozas, V., Olano, J.M., 2016a. Feedbacks between earlywood anatomy and non-structural carbohydrates affect spring phenology and wood production in ring-porous oaks. Biogeosciences 13, 5499–5510. http://dx.doi.org/10.5194/bg-13-5499-2016.

Pérez-de-Lis, G., Rossi, S., Vázquez-Ruiz, R.A., Rozas, V., García-González, I., 2016b. Do changes in spring phenology affect earlywood vessels? Perspective from the xylogenesis monitoring of two sympatric ring-porous oaks. New Phytol. 209, 521–530. http://dx.doi.org/10.1111/nph.13610.

Pérez-de-Lis, G., Olano, J.M., Rozas, V., Rossi, S., Vázquez-Ruiz, R.A., García-González, I., 2017. Environmental conditions and vascular cambium regulate carbon allocation to xylem growth in deciduous oaks. Funct. Ecol. 31, 592–603. http://dx.doi.org/10.1111/1365-2435.12789.

Polge, H., 1966. Établissement des courbes de variation de la densité du bois par exploration densitométrique de radiographies d'échantillons prélevés à la tarière sur des arbres vivants: applications dans les domaines Technologique et Physiologique. Ann. Sci. For. 23, 1–206. http://dx.doi.org/10.1051/forest/19660101.

R Core Team, 2016. R: A Language and Environment for Statistical Computing. URL. R Foundation for Statistical Computing, Vienna, Austria. https://www.R-project.org/.

Ren, P., Rossi, S., Gričar, J., Liang, E., Čufar, K., 2015. Is precipitation a trigger for the onset of xylogenesis in *Juniperus przewalskii* on the north-eastern Tibetan Plateau? Ann. Bot. 115, 629–639. http://dx.doi.org/10.1093/aob/mcu259.

Rigling, A., Waldner, P.O., Forster, T., Bräker, O.U., Pouttu, A., 2001. Ecological interpretation of tree-ring width and intraannual density fluctuations in *Pinus sylvestris* on dry sites in the central Alps and Siberia. Can. J. For. Res. 31, 18–31. http://dx.doi.org/10.1139/cjfr-31-1-18.

Rosner, S., Světlik, J., Andreassen, K., Børja, I., Dalsgaard, L., Evans, R., Karlsson, B., Tollefsruf, M., Solber, S., 2014. Wood density as a screening trait for drought sensitivity in Norway spruce. Can. J. For. Res. 44, 154–161. http://dx.doi.org/10.1139/cjfr-2013-0209.

Rossi, S., Deslauriers, A., Anfodillo, T., 2006. Assessment of cambial activity and xylogenesis by microsampling tree species: an example at the Alpine timberline. IAWA J. 27, 383–394. http://dx.doi.org/10.1163/22941932-90000161.

Rossi, S., Deslauriers, A., Gričar, J., Seo, J.-W., Rathgeber, C.B.K., Anfodillo, T., Morin, H., Levanic, T., Oven, P., Jalkanen, R., 2008. Critical temperatures for xylogenesis in conifers of cold climates. Glob. Ecol. Biogeogr. 17, 696–707. http://dx.doi.org/10.1111/j.1466-8238.2008.00417.x.

Rozas, V., García-González, I., Zas, R., 2011. Climatic control of intra-annual wood density fluctuations of *Pinus pinaster* in NW Spain. Trees 25, 443–453. http://dx.doi.org/10.1007/s00468-010-0519-5.

Schweingruber, F.H., 1988. Tree Rings. Springer, Netherlands, Dordrecth, Holland.

Speer, J.H., 2012. Fundamentals of Tree-Ring Research. The University of Arizona Press, Tucson, USA.

Stahle, D.W., Cleaveland, M.K., Grissino-Mayer, H.D., Griffin, R.D., Fye, F.K., Therrell, M.D., Burnette, D.J., Meko, D.M., Villanueva Diaz, J., 2009. Cool- and warm-season precipitation reconstructions over western New Mexico. J. Clim. 22, 3729–3750. http://dx.doi.org/10.1175/2008JCLI2752.1.

Vaganov, E., Hughes, M.K., Kirdyanov, A.V., Schweingruber, F.H., Silkin, P.P., 1999. Influence of snowfall and melt timing on tree growth in subarctic Eurasia. Nature 400, 149–151. http://dx.doi.org/10.1038/22087.

Vaganov, E., Anchukaitis, K., Evans, M., 2011. How well understood are the processes that create dendroclimatic records? A mechanistic model of the climatic control on conifer tree-ring growth dynamics. I. In: Hughes, M., Swetnam, T., Diaz, H. (Eds.), Dendroclimatology: Progress and Prospects. Springer, pp. 36–76.

Vaganov, E.A., Schulze, E.D., Skomarkova, M.V., Knohl, A., Brand, W.A., Roscher, C., 2009. Intra-annual variability of anatomical structure and δ13C values within tree rings of spruce and pine in alpine, temperate and boreal Europe. Oecologia 161, 729–745. http://dx.doi.org/10.1007/s00442-009-1421-y.

Vicente-Serrano, S.M., Azorin-Molina, C., Sanchez-Lorenzo, A., Morán-Tejeda, E., Lorenzo-Lacruz, J., Revuelto, J., López-Moreno, J.I., Espejo, F., 2013. Temporal evolution of surface humidity in Spain: recent trends and possible physical mechanisms. Clim. Dyn. 42, 2655–2674. http://dx.doi.org/10.1007/s00382-013-1885-7.

Vicente-Serrano, S.M., Beguería, S., López-Moreno, J.I., 2010. A multi-scalar drought index sensitive to global warming: the Standardized Precipitation Evapotranspiration Index–SPEI. J. Clim. 23, 1696–1718. http://dx.doi.org/10.1175/2009JCLI2909.1.

Vicente-Serrano, S.M., Camarero, J.J., Olano, J.M., Martín-Hernández, N., Peña-Gallardo, M., Tomás-Burguera, M., Gazol, A., Azorin-Molina, C., Bhuyan, U., El Kenawy, A., 2016. Diverse relationships between forest growth and the normalized difference vegetation index at a global scale. Remote Sens. Environ. 187, 14–29. http://dx.doi.org/10.1016/j.rse.2016.10.001.

Vieira, J., Campelo, F., Nabais, C., 2009. Age-dependent responses of tree-ring growth and intra-annual density fluctuations of *Pinus pinaster* to Mediterranean climate. Trees 23, 257–265. http://dx.doi.org/10.1007/s00468-008-0273-0.

Vieira, J., Campelo, F., Nabais, C., 2010. Intra-annual density fluctuations of Pinus pinaster are a record of climatic changes in the western Mediterranean region. Can. J. For. Res. 40, 1567–1575. http://dx.doi.org/10.1139/X10-096.

Vieira, J., Campelo, F., Rossi, S., Carvalho, A., Freitas, H., Nabais, C., 2015. Adjustment capacity of maritime pine cambial activity in drought-prone environments. PLoS One 10, e0126223. http://dx.doi.org/10.1371/journal.pone.0126223.

Vieira, J., Rossi, S., Campelo, F., Freitas, H., Nabais, C., 2014. Xylogenesis of *Pinus pinaster* under a Mediterranean climate. Ann. For. Sci. 71, 71–80. http://dx.doi.org/10.1007/s13595-013-0341-5.

von Arx, G., Arzac, A., Fonti, P., Frank, D., Zweifel, R., Rigling, A., Galiano, L., Gessler, A., Olano, J.M., 2017. Responses of sapwood ray parenchyma and non-structural carbohydrates of *Pinus sylvestris* to drought and long-term irrigation. Funct. Ecol. 31, 1371–1382. http://dx.doi.org/10.1111/1365-2435.12860.

Wigley, T.M.L., Briffa, K.R., Jones, P.D., 1984. On the average value of correlated time series, with applications in dendroclimatology and hydrometeorology. J. Clim. Appl. Meteorol. 23, 201–213.

Wilkinson, S., Ogée, J., Domec, J.C., Rayment, M., Wingate, L., 2016. Biophysical modelling of intra-ring variations in tracheid features and wood density of *Pinus pinaster* trees exposed to seasonal droughts. Tree Physiol. 35, 305–318. http://dx.doi.org/10.1093/treephys/tpv010.

Zalloni, E., de Luis, M., Campelo, F., Novak, K., DeMicco, V., Di Filippo, A., Vieira, J., Nabais, C., Rozas, V., Battipaglia, G., 2016. Climatic signals from intra-annual density fluctuation frequency in Mediterranean pines at a regional scale. Front. Plant Sci. 7, 579. http://dx.doi.org/10.3389/fpls.2016.00579.